

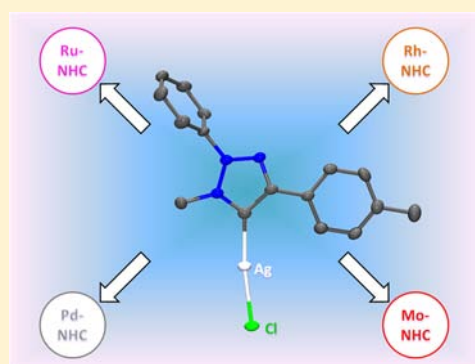
# Exploring the Scope of a Novel Ligand Class: Synthesis and Catalytic Examination of Metal Complexes with 'Normal' 1,2,3-Triazolylidene Ligands

Lars-Arne Schaper,<sup>†</sup> Lilian Graser,<sup>†</sup> Xuhui Wei, Rui Zhong, Karl Öfele, Alexander Pöthig, Mirza Cokoja, Bettina Bechlars, Wolfgang A. Herrmann,\* and Fritz E. Kühn\*

Chair of Inorganic Chemistry/Molecular Catalysis, Catalysis Research Center, Technische Universität München, Ernst-Otto-Fischer-Strasse 1, D-85747 Garching bei München, Germany

## Supporting Information

**ABSTRACT:** Using new 'normal'-substituted 1,2,3-triazolylidene silver compounds as starting materials allowed for preparation of a series of molybdenum, ruthenium, rhodium, and palladium transition metal complexes bound to the new 1,2,3-triazolylidene ligand system. In this work, the first triazolylidene Mo compound is presented as well as the first structural investigation of a silver complex with a monodentate 1,2,3-triazolylidene. Furthermore, the triazolylidene Pd complex and the Mo complex were tested as precatalysts in Suzuki–Miyaura coupling and epoxidation catalysis, respectively.



## INTRODUCTION

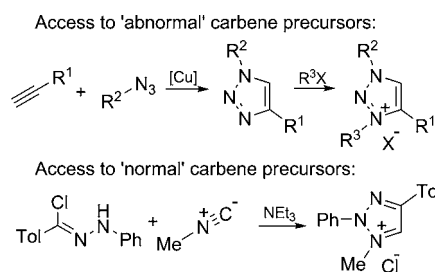
After the isolobal analogy between *N*-heterocyclic carbenes (NHCs) and phosphines<sup>1</sup> was discovered, research on utilization of NHCs as ligands in transition metal complexes experienced an enormous boost.<sup>2</sup> The first report on the catalytic activity of NHC–metal complexes<sup>3</sup> had a great impact on development of NHC-ligated homogeneous catalysts for a plethora of organic reactions. To date, not only have extremely weak NHC donors been identified, i.e., tetrazolylidene ligands,<sup>4</sup> but also highly nucleophilic examples were synthesized.<sup>5</sup> The first evidence of alternative, abnormal binding modes of imidazolylidene ligands led to an amplified interest in donor strength variation of this ligand class.<sup>6</sup>

A young but steadily growing family of rather strong NHC sigma donors are 1,2,3-triazolylidenes, which are by definition considered to reveal an 'abnormal' binding mode due to their 1,3,4-substitution pattern.<sup>7</sup> After their initial discovery by Albrecht and co-workers and after isolation of the first free stable carbene congeners of this NHC class by Bertrand's group,<sup>8</sup> a plethora of new compounds equipped with 1,2,3-triazolylidenes was characterized, reflecting strong recent interest of the scientific community.<sup>9</sup> The growing significance of triazolylidene ligands may be justified by their great potential for catalytic applications<sup>10</sup> as well as by their interesting zwitterionic behavior.<sup>11</sup>

In spite of the growing significance of 'abnormal' 1,2,3-triazolylidenes (exhibiting a 1,3,4-substitution pattern), examples of 'normal' congeners with a 1,2,4-substitution pattern are extremely rare. Only recently, our group reported 'normal'

1,2,3-triazolylidene compounds featuring a 1,2,4-substitution pattern.<sup>12</sup> Synthesis of the corresponding precursor salts does not follow the established Cu-catalyzed click chemistry routes but proceeds via a ring-closing procedure based on isocyanides and hydrazonoylchlorides (Scheme 1).<sup>13</sup> Apart from the

### Scheme 1. Traditional Access to 1,3,4-Substituted 1,2,3-Triazolylidenes<sup>8</sup> and Recently Described Access to Their 1,2,4-Substituted Relatives, 'Normal' 1,2,3-Triazolylidenes<sup>12</sup>



unprecedented behavior of the first triazolylidene–ammonia adduct, this underexplored carbene class also revealed high  $\sigma$ -donor strength when examined in the  $[\text{Ir}(\text{CO})_2\text{CIL}]$  system. In addition to the higher  $\sigma$  electron donation, the unsymmetrical substitution pattern of our triazolylidene ligand may even leverage benefits in enantioselective catalysis.

Received: March 2, 2013

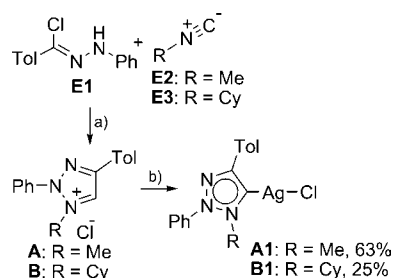
Published: May 6, 2013

This work aims at enlarging the family of new ‘normal’ triazolylidene carbene ligands by exploring the silver carbene access route in order to yield new examples of metal complexes with differently substituted ligands. Furthermore, the catalytic potential of this ligand class is examined.

## RESULTS AND DISCUSSION

**Synthesis of Ag–NHC Complexes.** Precursor salts applied in this work were synthesized from hydrazonoyl-chloride **E1**<sup>14</sup> and isocyanides **E2**<sup>15</sup> or **E3**<sup>16</sup> (Scheme 2). With

**Scheme 2. Synthesis of Methyl- and Cyclohexyl-Substituted Triazolium Chlorides A and B As Described by Moderhack et al.<sup>13</sup> and Subsequent Synthesis of Corresponding Silver Complexes A1 and B1<sup>a</sup>**



<sup>a</sup>Reaction conditions: (a) 1.00 equiv of NEt<sub>3</sub>, RT, 24 h, MeCN. (b) For **A1** 0.50 equiv of Ag<sub>2</sub>O, RT, exclusion of light, 2 h, DCM. For **B1**: 1.50 equiv of Ag<sub>2</sub>O, molecular sieves, RT, exclusion of light, 18 h, MeCN:DCM/1:1.

the starting materials synthesized, the ensuing ring-closing reaction allowed for isolation of 1-methyl-2-phenyl-4-tolyl-1,2,3-triazolium chloride **A** or 1-cyclohexyl-2-phenyl-4-tolyl-1,2,3-triazolium chloride **B**. According to the literature, however, this method remains limited to generation of 1-alkyl-substituted triazolium salts. In order to generate the

corresponding Ag complexes as viable carbene transfer reagents, the precursor triazolium salts were treated with Ag<sub>2</sub>O according to Wang and Lin.<sup>17</sup> Using methyl-substituted **A**, synthesis of Ag compound **A1** proceeds analogously to frequently applied reaction conditions in reasonable yields (Scheme 2).

The reactivity of the cyclohexyl-substituted triazolium salt **B** was different. The Ag complex could not be generated by applying the same reaction conditions as for **A1**, and only complex mixtures were isolated. After studying a variety of solvents and conditions, the optimum reaction conditions could be identified but only allowed for synthesis of **B1** in rather low yields. The red color of the reaction solution, however, is an indication of triazolium ring decomposition. Accurate characterization of both isolated compounds led to unambiguous identification as carbene compounds. First evidence was provided by <sup>1</sup>H NMR spectroscopy. The proton resonances, which are characteristic for triazolium salts (proton bound to C5, 11.25 ppm for **A** [CDCl<sub>3</sub>], 11.79 ppm for **B** [CDCl<sub>3</sub>]), disappeared after reaction with silver oxide. Furthermore, the signal for the methyl group bound to N1 was shifted upfield from 4.78 ppm in **A** (CDCl<sub>3</sub>) to 4.29 ppm in **A1** (CDCl<sub>3</sub>). In addition, the resonance for the proton bound to the ipso-C of the cyclohexyl moiety was shifted upfield from 4.52 ppm in **B** (CDCl<sub>3</sub>) to 4.36 ppm in **B1** (CDCl<sub>3</sub>), with both shifts indicating subtle changes in the electronic environments of the heterocycles. In both cases, <sup>13</sup>C{<sup>1</sup>H} NMR gave further hints for carbene formation, as characteristic downfield signals were observed at 170.6 ppm (CDCl<sub>3</sub>) for **A1** and 163.80 ppm (CDCl<sub>3</sub>) for **B1**. In general, observation of a carbene resonance suggests nonfluxional behavior (i.e., no alternating between mono- and bis(carbene) Ag species [AgCl(NHC)] and [Ag(NHC)<sub>2</sub>]<sup>+</sup>[AgCl<sub>2</sub>]<sup>-</sup>).<sup>18</sup> However, for **A1** we were not able to confirm preference for one of these structures by mass spectroscopy, since under FAB conditions a mixture of **A**, [Ag(A<sub>carb</sub>)]<sup>+</sup>, and [Ag(A<sub>carb</sub>)<sub>2</sub>]<sup>+</sup> was observed. The same behavior was observed for **B1**.

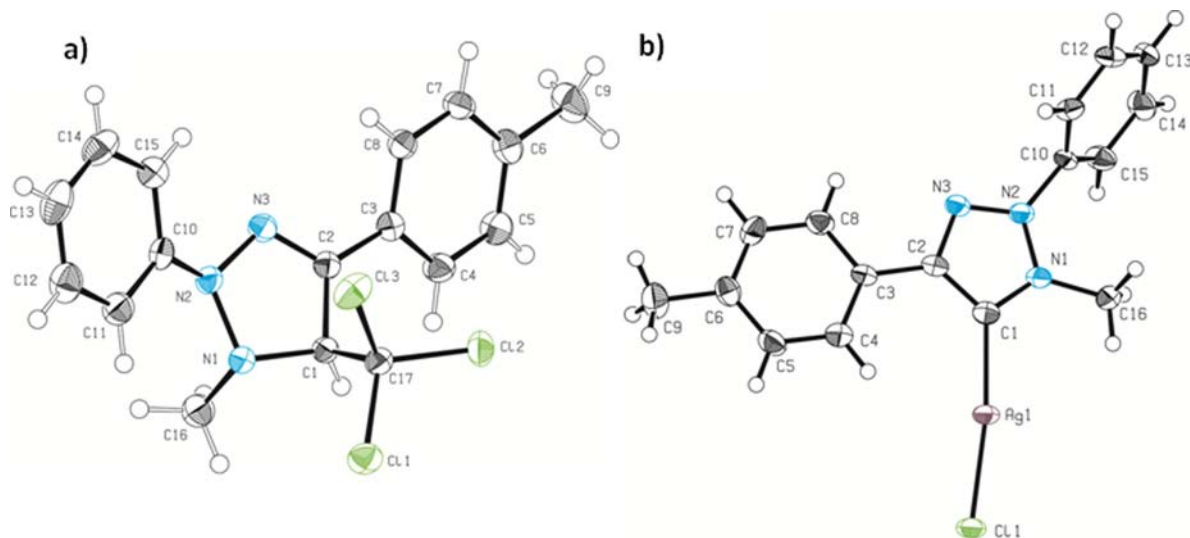


**Figure 1.** ORTEP representation of (a) observed triazolylidene chloroform adduct (thermal ellipsoids are shown at a probability level of 50%). Selected bond distances [Å] and angles [deg]: C1–C17 1.551(2), N1–C1 1.464(2), N3–C2 1.288(2), N2–N3 1.376(2), N1–N2 1.456(2), N1–C1–C2 102.8(1). Torsion angles [deg]: N3–N2–N1–N16 111.16(13), N2–N1–C1–C17 108.80(12). (b) Linear triazolylidene Ag complex **A1** (thermal ellipsoids are shown at a probability level of 50%). Selected bond distances [Angstroms] and angles [degrees]: Ag1–Cl1 2.335(1), Ag1–C1 2.084(4), N1–N2 1.361(4), N1–C1 1.332(4), N2–N3 1.321(3), N3–C2 1.340(4); Cl1–Ag1–C1 172.5(1), N1–C1–C2 102.9(3). Torsion angle [degrees]: N3–N2–N1–C16 4.3(3).

The first crystallization attempts of **A1** revealed interesting behavior of the compound in  $\text{CHCl}_3$  solution. Instead of isolating single crystals of **A1**, we obtained crystals of the chloroform adduct of free carbene **A** (Figure 1). Although similar examples for adducts of saturated NHCs and chloroform exist,<sup>19</sup> triazolylidene examples of these compounds have not been described and structural representations were also not published before. Isolation of this type of potential carbene precursor from a silver carbene is certainly not cost efficient but provides a new alternative to the known access routes. For directed synthesis of this chloroform adduct, we heated a  $\text{CDCl}_3$  solution of **A1** in NMR scale experiments and monitored the reaction by  $^1\text{H}$  NMR. No single product could be observed, but in turn we saw mixtures of at least five different products. ESI-MS suggested that the chloroform adduct was obtained in traces only (4% in Supporting Information). However, we did not focus on further elaboration of this synthesis.

The crystal structure underlines the nonaromatic bond character within the chloroform adduct's heterocycle [C1–N1 1.464(2) Å, N3–C2 1.288(2) Å, N2–N3 1.376(2) Å, N1–N2 1.456(2) Å]. The value for the N1–N2 bond is astonishingly long compared to the single bond in hydrazine<sup>20</sup> but in line with observations made for the ammonia adduct [N1–N2 1.457(2) Å] published by our group.<sup>12</sup> Furthermore, the other values are in good accordance to the values obtained for the earlier described ammonia adduct [C1–N1 1.483(2) Å, N3–C2 1.287(2) Å, N2–N3 1.383(2) Å].<sup>12</sup> Here, the shortened C1–N1 bond length in the chloroform adduct gives evidence for the increased electron density at C1 because of the  $-\text{CCl}_3$  substituent. The torsion angle observed for N3–N2–N1–C16 [111.16(13)°] of the chloroform adduct supports this observation when compared to N3–N2–N1–C16 [131.20(15)°] of the ammonia adduct.

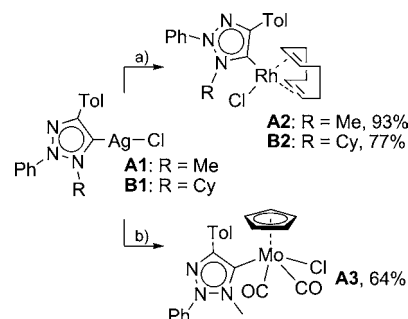
By avoiding chloroform as solvent, single crystals suitable for X-ray diffraction were grown by slow evaporation of a saturated dichloromethane (DCM) solution of **A1**. Figure 1 depicts the crystal structure of **A1**, which is, to the best of our knowledge, the first structural characterization of a mono-1,2,3-triazolylidene-ligated Ag complex.<sup>9f</sup>

In contrast to many structurally characterized imidazolylidene silver complexes, **A1** does not form polymeric or cluster structures in the solid state.<sup>2f,9f,21</sup> The Ag...Ag distance of 3.414(1) Å lies just within the sum of the van der Waals radii of both ions,<sup>22</sup> implying only weak argentophilic interactions.<sup>17,23</sup> The crystal structure provides strong evidence that at least at room temperature the mono-carbene species  $[\text{Ag}(\text{A}_{\text{carb}})\text{Cl}]$  is preferred over  $[\text{Ag}(\text{A}_{\text{carb}})_2]^+[\text{AgCl}_2]^-$  or  $[\text{Ag}(\text{A}_{\text{carb}})_2]^+\text{Cl}^-$ . Furthermore, the crystallographic data of **A1** corroborate the expected 'normal' 1,2,3-triazolylidene structure, featuring a 1,2,4-substitution pattern. Selected bond distances between heterocyclic ring atoms (see caption of Figure 1) are nearly equidistant, suggesting a conjugated ring system. In comparison to the triazolylidene chloroform adduct, the N1–N2 bond distance is now considerably shortened [1.361(4) Å]. A conjugated ring system is further evidenced by a very flat C1–N1–N2–C16 torsion angle of 4.8(3)°, contrasting the angle of 59.1° observed in the already published structure of the nonconjugated ammonia adduct.<sup>12</sup> The angle N1–C1–C2 of 102.9(3)° around the carbene carbon and its closest ring members corresponds well to that observed in the abnormal 1,2,3-triazolylidene Pd complex analyzed by Albrecht et al.<sup>8a</sup> [N1–C1–C2 103.0(12)°]. Compound **A1** reveals a slightly

bent linear structure with an C1–Ag1–Cl1 angle of 172.5(1)°. Compared to other linear gold chloride compounds presented by Crowley et al.<sup>10b</sup> [177.2(1)°] and by our group [177.1(2)°],<sup>12</sup> this deviation from an ideal linear structure is slightly more pronounced. The C1–Ag1 bond distance of 2.084(4) Å is elongated compared to the analogous gold compound [1.997(6) Å].<sup>12</sup> Nevertheless, it is in line with the row of imidazolylidene–AgCl compounds presented by Nolan et al.<sup>23</sup> [2.056–2.094 Å]. On the basis of the observations made for **A1**, we assume that cyclohexyl congener **B1** will also primarily exist in the mono-carbene complex form, since its increased steric demand will further reduce dimerization tendencies.

**Synthesis of Rh- and Mo-Triazolylidene Complexes by Transmetalation.** Rhodium complexes **A2** and **B2** were obtained in excellent yields by application of the respective Ag compound as carbene transfer reagent (Scheme 3). Reaction with dimeric precursor  $[\text{Rh}(\text{COD})\text{Cl}]_2$  proceeds smoothly to completion within 2 h at room temperature.

**Scheme 3. Syntheses Starting from Silver Carbenes **A1** and **B1**, Yielding the Corresponding Triazolylidene Rh and Mo Complexes **A2**, **B2**, and **A3**<sup>a</sup>**



<sup>a</sup>Reaction conditions: (a) For **A1** and **A2** 0.50 equiv of  $[\text{Rh}(\text{COD})\text{Cl}]_2$ , RT, exclusion of light, 2 h, DCM; (b) only for **A1** 1.00 equiv of  $[\text{Mo}(\text{CO})_3\text{CpCl}]$ , 45 °C, exclusion of light, 16 h, DCM.

Since the compound was earlier described by isolation following an alternative access route,<sup>12</sup> we were able to identify **A2** by checking agreement with spectroscopic data. In the case of **B2**,  $^1\text{H}$  NMR suggested emergence of a new carbene complex by a notable downfield shift of one of the toluene aryl signals from 8.10 ppm in **A2** ( $\text{CD}_2\text{Cl}_2$ ) to 8.80 ppm in **B2** ( $\text{CDCl}_3$ ). Additionally, in the  $^{13}\text{C}\{^1\text{H}\}$  NMR spectrum, the carbene carbon peak appears as a doublet at 181.1 ppm ( $^1J_{\text{Rh-C}} = 45.7$  Hz), suggesting C1–Rh coordination. Single crystals of **B2** suitable for X-ray diffraction were grown by slow diffusion of pentane into a saturated solution of the complex in chloroform. An ORTEP representation of the obtained crystal structure of **B2** is shown in Figure 2. According to a C1–Rh1–Cl1 angle of 89.25(5)°, the symmetry of **B2** is close to an ideal square-planar coordination of the Rh center. The torsion angle of N3–N2–N1–C16 (179.42°) is extremely flat, indicating even higher convergence to an ideal conjugated heterocyclic ring system than in **A1**. The C1–Rh1 bond distance of 2.030(2) Å is very similar to the abnormal triazolylidene Rh complex presented by Albrecht et al.<sup>8a</sup> [2.027(6) Å]. Analogously, the Rh1–Cl1 bond length in our compound **B2** [2.388(1) Å] resembles the bond length in Albrecht's triazolylidene Rh compound [2.372(1) Å]. The Rh–C<sub>carbene</sub> bond distance values observed for the abnormal bis(1,2,3-

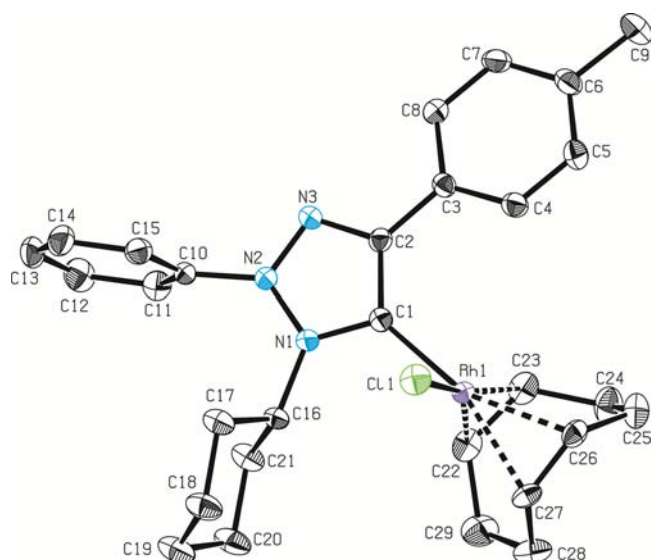


**Figure 2.** ORTEP representation of the crystal structure data of **B2** (thermal ellipsoids are shown at a probability level of 50%). Selected bond distances [Angstroms] and angles [degrees]: Rh1–C1 2.030(2), Rh1–Cl1 2.3877(5); Cl1–Rh1–C1 89.25(5), N1–C1–C2 102.7(1). Torsion angle [degrees]: N3–N2–N1–C16 179.4(2).

triazolylidene) Rh compound structurally characterized by Bertrand and co-workers [2.071(4) and 2.068(4) Å] are slightly elongated, certainly attributable to their rigid bis(carbene) ligand design.<sup>9e</sup>

[Mo(CO)<sub>3</sub>CpCl] was reacted with **A1** and gave the air- and moisture-stable complex **A3** in good yields (Scheme 3). Complex **A3** is highly soluble in polar solvents such as acetonitrile, DCM, or chloroform as well as in less polar solvents such as benzene and toluene. It even exhibits partial solubility in diethyl ether, which proved to be an ideal solvent for recrystallization. To the best of our knowledge, we isolated the first example of a group 6 metal coordinated to a 1,2,3-triazolylidene. In contrast to the earlier published access route to related compounds,<sup>24</sup> relatively mild reaction conditions were applied (40 °C, 16 h). Formation of a new compound was confirmed by <sup>1</sup>H NMR with the shift of the Cp signals from 5.66 (CDCl<sub>3</sub>) to 5.13 ppm (CD<sub>2</sub>Cl<sub>2</sub>). Furthermore, in the <sup>13</sup>C{<sup>1</sup>H} NMR spectrum only two carbonyl signals with the same intensity could be observed at 258.8 and 253.2 ppm as well as a characteristic carbene signal at 185.8 ppm. Further evidence was provided by the IR spectrum, which showed a strong shift for the carbonyl resonances, from 1964 and 2056 cm<sup>-1</sup> in [Mo(CO)<sub>3</sub>CpCl] to 1944 and 1848 cm<sup>-1</sup> in **A3**.<sup>25</sup> Comparison to the elevated IR resonances in the analogous dibenzylimidazolylidene compound [Mo(CO)<sub>2</sub>CpCl(IBz)] (**IBzMo**) [1953 and 1872 cm<sup>-1</sup> (KBr)] described by Hor and Zhao<sup>24</sup> indicates that in **A3** increased electron density is present at the metal center, suggesting the presence of the stronger electron-donating triazolylidene. Single crystals suitable for X-ray diffraction could be grown at 5 °C from a saturated solution of **A3** in diethyl ether. Spectroscopic data obtained allows for comparison to the structure of **IBzMo** (Figure 3).<sup>24</sup> Interestingly, the differences in the carbene ligands are not reflected in the Mo–C<sub>carbene</sub> bond length [2.221(4) Å in **A3** vs 2.221(3) Å in **IBzMo**]. Also, the average bond lengths between Mo and both carbonyl ligands are more

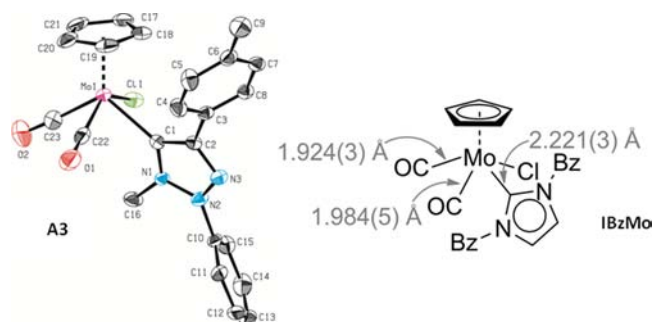


**Figure 3.** ORTEP representation of the crystal structure data of **A3** (thermal ellipsoids are shown at a probability level of 50%). Selected bond distances [Angstroms] and angles [degrees]: Mo1–C1 2.221(4), Mo1–C22 1.965(4), Mo1–C23 1.945(4), Mo1–Cl1 2.519(1), C1–Mo1–C22 74.61(17), C1–Mo1–C23 113.3(2). Bond lengths for **A3** and **IBzMo**<sup>24</sup> are within the limits of triple standard deviation; hence, no absolute differences can be determined.

or less similar in both compounds (1.955 Å for **A3** and 1.954 Å for **IBzMo**, Figure 3).

In the case of cyclohexyl-substituted silver triazolylidene **B1**, no Mo complex could be isolated, although the same reaction conditions were applied as in the case of **A3**. Formation of a supposed product was observable in <sup>1</sup>H NMR, with a characteristic shift of the Cp signals. However, only complex mixtures were obtained.

**Epoxidation Catalysis.** Use of complexes of the general type [Mo(η<sup>5</sup>-C<sub>5</sub>R<sub>5</sub>)O<sub>2</sub>X] in the epoxidation of olefins is well established and has been extensively studied throughout the last three decades.<sup>26</sup> Several groups showed that carbonyl precursors of general formula [Mo(η<sup>5</sup>-C<sub>5</sub>R<sub>5</sub>)(CO)<sub>3</sub>X] can be directly used as catalyst precursors in the homogeneous epoxidation of olefins.<sup>27</sup> For these reasons, complex **A3** was tested as catalyst for epoxidation of several internal and terminal alkenes using *tert*-butyl hydroperoxide (TBHP, 5.5 M decane solution) as oxidant. Using cyclooctene as substrate, optimal reaction conditions regarding solvent, temperature, oxidant, and catalyst loading were evaluated. Results of the solvent and temperature screening are summarized in Table 1.

**Table 1.** Epoxidation of Cyclooctene Utilizing **A3** As Precatalyst<sup>a</sup>

solvent	yield [%] <sup>c</sup> after 4 h (24 h)	
	25 °C	55 °C
CHCl <sub>3</sub> <sup>b</sup>	24 (28)	27 (35)
CH <sub>3</sub> CN <sup>b</sup>	25 (29)	31 (36)
toluene <sup>b</sup>	19 (22)	25 (36)
decane <sup>b</sup>	32 (53)	38 (52)
THF <sup>b</sup>	<10 (<10)	<10 (<10)
MeOH <sup>b</sup>	<10 (<10)	<10 (<10)
[C <sub>4</sub> mim] <sup>+</sup> Cl <sup>-b</sup>	41 (85)	55 (85)
[C <sub>4</sub> mim] <sup>+</sup> [BF <sub>4</sub> ] <sup>-b</sup>	46 (88)	64 (88)
[C <sub>4</sub> mim] <sup>+</sup> [NTf <sub>2</sub> ] <sup>-b</sup>	45 (91)	52 (91)
[C <sub>8</sub> mim] <sup>+</sup> [NTf <sub>2</sub> ] <sup>-b</sup>	43 (96)	74 (96)

<sup>a</sup>Effects of solvent and temperature variation on conversion are displayed. <sup>b</sup>Reactions were carried out using a ratio for catalyst:substrate:oxidant of 1:100:200. <sup>c</sup>Yield determined by GC.

Comparison of different reaction media showed that the highest conversions can be obtained using ionic liquid  $[\text{C}_8\text{mim}]^+[\text{NTf}_2]^-$  at 55 °C ( $\text{C}_8\text{mim}$  = 1-methyl-3-octylimidazolium;  $\text{NTf}_2^-$  = bis(trifluoromethanesulfonyl)imide). No conversion of epoxide could be observed, neither in THF nor in methanol, reflecting the coordinative nature of these solvents, as observed earlier.<sup>28</sup> Therefore, all further experiments were carried out in  $[\text{C}_8\text{mim}]^+[\text{NTf}_2]^-$  at 55 °C.

In all organic solvents, except for decane, the red color of the reaction solution disappeared after 20 min and a fine, yellow precipitate formed. Hor et al.<sup>24</sup> observed an analogous behavior for imidazolylidene-based precatalysts. The precipitate was found to be soluble in DMSO only and characterized by IR,  $^1\text{H}$  NMR, and ESI-MS. In the  $^1\text{H}$  NMR the Cp resonance at 5.1 ppm disappeared and a set of peaks at 3.7, 7.3, and 8.6 ppm could be observed, which most likely represents decomposition products of the Cp and triazolium ligands. Strong absorptions in the IR spectrum around  $950\text{ cm}^{-1}$  and  $800\text{ cm}^{-1}$  indicate several Mo=O vibration bands. The negative mode of the ESI-MS spectrum shows different  $[\text{Mo}_n\text{O}_x]^{-y}$  species, as observed in Hor's work. By combining these results it was not possible to fully interpret the nature of the solid based on the available data. However, it is most likely that a  $[\text{triazolium}]^+[\text{Mo}_n\text{O}_x]^{-y}$  species forms, just as presumed earlier.<sup>24</sup>

Comparison between catalysis in  $\text{CH}_2\text{Cl}_2$  and in the ionic liquid (IL)  $[\text{C}_8\text{mim}]^+[\text{NTf}_2]^-$  shows that the activity of the formed catalyst species is higher in the IL. Kinetic evaluations were undertaken for epoxidation of cyclooctene in MeCN and  $[\text{C}_8\text{mim}]^+[\text{NTf}_2]^-$  (Figure 4). Here, acetonitrile was chosen as

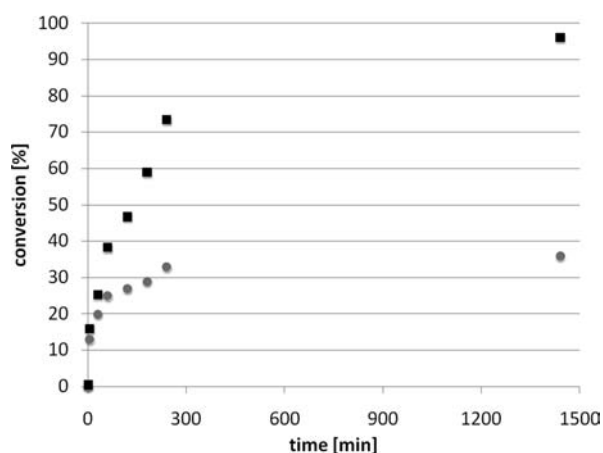


**Figure 4.** Kinetic profile for conversion of cyclooctene with TBHP (in decane) at 55 °C using complex A3 as the catalyst precursor. Results for epoxidation catalysis using MeCN as solvent (solid gray symbol) or  $[\text{C}_8\text{mim}]^+[\text{NTf}_2]^-$  (■).

solvent to allow for better comparison to the results obtained in related investigations.<sup>24</sup> As shown in Figure 4, conversion of cyclooctene reaches its maximum at around 35% when using MeCN as a solvent, while in the IL epoxidation continues and a conversion of 96% after 24 h is reached. Apparently, the polar environment of the ionic liquid supports the emerging active catalyst species, since no precipitate of Mo salts appears, as observed in MeCN.<sup>24</sup>

Although compound A3 shows moderate catalytic activity only, it still appears to be slightly more active than the related *ansa*-bridged Cp-functionalized NHC complexes.<sup>29</sup> In order to compare the catalytic activity of A3 with the related

imidazolylidene-based systems  $[\text{MoBr}(\text{CO})_2\text{Cp}(\text{NHC})]$  reported by Hor et al.,<sup>24</sup> we synthesized the analogous chloride compound  $[\text{Mo}(\text{CO})_2\text{CpCl}(\text{IMes})]$  following published procedures. Catalytic yields were slightly higher for the triazolylidene-based system in MeCN as well as in  $[\text{C}_8\text{mim}]^+[\text{NTf}_2]^-$  (see Supporting Information for synthetic and catalytic details).

Apart from testing the catalytic performance of A3 in epoxidation of cyclooctene as standard reaction, we were also interested in finding its limitations in terms of substrate scope. For that purpose, more challenging starting materials were chosen for catalytic examination. Although conversions were low compared to the more reactive cyclooctene, moderate yields could be obtained for epoxidation of 1-octene, *trans*- $\beta$ -methylstyrene, and *cis*-stilbene (Table 2) in  $[\text{C}_8\text{mim}]^+[\text{NTf}_2]^-$ .

**Table 2.** Epoxidation of Various Substrates Utilizing A3 As Precatalyst<sup>a</sup>

substrate	yield after 4 h (24 h) [%] <sup>b</sup>
1-octene	43 (65)
<i>trans</i> - $\beta$ -methylstyrene	24 (32)
<i>cis</i> -stilbene	38 (54)

<sup>a</sup>Effects of solvent and temperature variation on conversion. <sup>b</sup>All reactions were carried out using a catalyst:substrate:oxidant ratio 1:100:200 at a reaction temperature of 55 °C; yields determined by NMR.

In order to probe the convenience of catalyst recycling in an ionic liquid-based system as well as to test the stability of the catalytic species, recycling experiments were undertaken in  $[\text{C}_8\text{mim}]^+[\text{NTf}_2]^-$ . For this purpose, after one catalytic run the upper solvent phase containing the product was removed from the catalyst/IL phase by addition of 5 mL of *n*-hexane and removal of the upper phase by cannulation and subjected to workup procedures and GC analysis (see the Experimental Section). Subsequently, a further batch of substrate and oxidants was added to the remaining IL phase. Evaluation of these recycling experiments suggests high stability of the catalytically active species, since the observed conversions remained comparably stable for six subsequent 24 h runs (Figure 5).

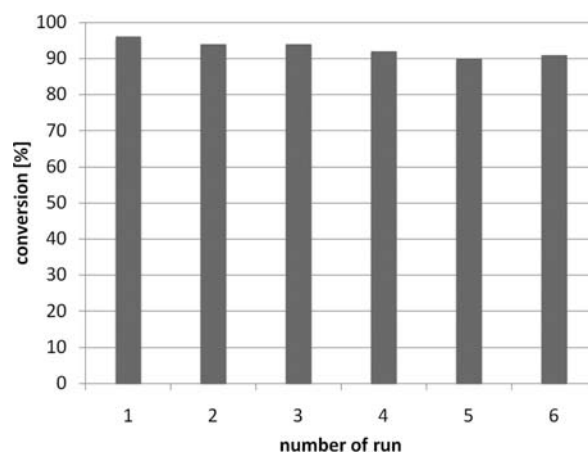
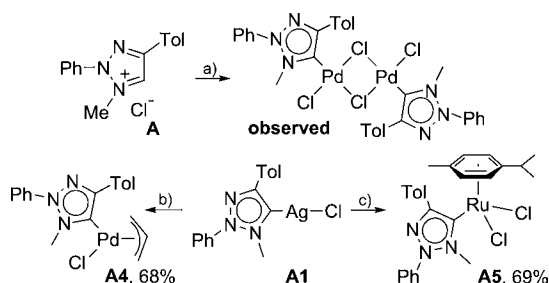


**Figure 5.** Epoxide yield for 6 cycles after 24 h reaction time applying A3 as catalyst. Cyclooctene was used as substrate and  $[\text{C}_8\text{mim}]^+[\text{NTf}_2]^-$  as solvent at a reaction temperature of 55 °C.

The preceding paragraphs showed that the catalytically active species derived from compound **A3** has moderate catalytic activity in a variety of olefin substrates as well as in recycling experiments. However, due to the observed precipitate formation, presumably a catalytically active Mo–polyoxo salt, it seems that system **A3** is not stable under oxidative conditions, and further examination will be necessary to reveal the intrinsically active catalyst system. Nevertheless, it is important to continue the search for more stable NHC-based oxidation catalyst systems, which are less prone to decomposition, as these could be capable of controlling the stereoselectivity in epoxidation products.

**Synthesis of Ru and Pd Complexes Bearing 1,2,3-Triazolylidene Ligands.** Since the cyclohexyl triazolylidene Ag complex **B1** seems to exhibit only limited applicability in carbene transfer reactions, further examinations focused on methyl-substituted **A1**. As to date no examples for group 8 and group 10 complexes bound to normal 1,2,3-triazolylidene ligands are known, we tested the carbene transfer reaction with **A1** and common dimeric metal complexes  $[\text{Pd}(\text{allyl})\text{Cl}]_2$  and  $[\text{Ru}(p\text{-cymene})\text{Cl}_2]_2$ . Reactions with both precursors were conducted at room temperature and allowed for facile isolation of triazolylidene-substituted Pd–allyl complex **A4** and the related triazolylidene cymene Ru dichloride compound **A5** in good yields (Scheme 4). Both compounds exhibit good stability to air and moisture.

**Scheme 4. Synthesis of New Pd and Ru Complexes with Methyl-Substituted Triazolylidene Ligands<sup>a</sup>**



<sup>a</sup>Reaction conditions: (a) 0.25 equiv of  $[\text{Pd}(\text{OAc})_2]$ ,  $-78^\circ\text{C}$  to RT, 16 h, THF; (b) 0.50 equiv of  $[\text{Pd}(\text{allyl})\text{Cl}]_2$ , RT, exclusion of light, 16 h, DCM; (c) 0.50 equiv of  $[\text{RuCl}_2(p\text{-cymene})]_2$ , RT, exclusion of light, 2 h, DCM.

In order to examine further access routes to metal complexes with normal triazolylidenes, we tested reaction of triazolium precursor **A** and  $[\text{Pd}(\text{OAc})_2]$ , one of the most common paths to generating Pd NHC complexes (Scheme 4). However, published procedures at elevated temperatures did not yield the desired product. Instead, a reaction protocol starting at  $-78^\circ\text{C}$  had to be applied in order to generate a Cl-bridged homo-bimetallic Pd triazolylidene complex. Single crystals of the Cl-bridged homo-bimetallic Pd complex depicted in Scheme 4 could be grown by slow diffusion of pentane into a saturated  $\text{CHCl}_3$  solution of the complex. An ORTEP representation of the structural data obtained for this compound is depicted in Figure 6a. The observed angles for  $\text{Cl1-Pd1-Cl1}$  [ $88.15(6)^\circ$ ] and  $\text{Cl2-Pd1-Cl1}$  [ $91.97(6)^\circ$ ] prove that the Pd compound exhibits an almost ideal quadratic planar structure. The Pd carbene bond [ $\text{C1-Pd1}$  1.963(2) Å] is in good accordance with the data provided for the row of I-bridged Pd compounds presented by Albrecht et al. [between 1.96(3) and 1.977(13)

Å].<sup>9c</sup> The Pd–Cl bond length of the nonbonding Cl [ $\text{Pd1-Cl1}$  2.2781(7) Å] is slightly shortened in comparison to Cl-bridged saturated NHC homo-bimetallic Pd compound reported by Chen, Liu, and co-workers [2.298(1) Å].<sup>30</sup> Since the obtained yield in the synthesis of the observed bimetallic Pd species was very low and rarely reproducible, we applied a different Pd precursor for subsequent synthetic attempts.

The existence of compound **A4** was quickly confirmed by identification of a new set of signals for the allyl ligand via  $^1\text{H}$  NMR spectroscopy as well as a characteristic carbene signal at 174.8 ppm ( $\text{CDCl}_3$ ). Furthermore, crystals suitable for X-ray diffraction were grown by slow diffusion of pentane into a saturated solution of **A4** in chloroform. The structure of complex **A4** could be confirmed (Figure 4b), but unfortunately, the comparatively low quality of the crystal prevents further discussion of structural parameters. Successful synthesis of the Ru complex **A5** was evidenced by characteristic new signals for the *p*-cymene ligand in the  $^1\text{H}$  NMR and a distinct carbene signal in the  $^{13}\text{C}\{^1\text{H}\}$  NMR spectrum (173.4 ppm in  $\text{CDCl}_3$ ). Further evidence was provided by elemental analysis. In an attempt to analyze the structure of **A5** by means of X-ray crystallography, only crystals of the metal precursor  $[\text{Ru}(p\text{-cymene})\text{Cl}_2]_2$  were found, indicating reduced stability of **A5** dissolved in chloroform under ambient light for days, as observed for the Ag compound **A1**.

**Suzuki–Miyaura Coupling Catalysis.** The catalytic activity of Pd precatalyst **A4** in C–C cross-coupling reactions was examined. A standard method to test the potential of Pd catalysts is the Suzuki–Miyaura reaction. Accordingly, the rare reports dealing with catalytic examinations of new ‘abnormal’ 1,2,3-triazolylidene Pd complexes explore their catalytic ability in this type of coupling reaction.<sup>31</sup> Albrecht et al.<sup>9j</sup> synthesized and tested 1,2,3-triazolylidene-substituted PEPPSI-type Pd catalysts, while Fukuzawa et al.<sup>9j</sup> examined Pd allyl, crotyl, and cinnamyl compounds bound to ‘abnormal’ 1,2,3-triazolylidenes,<sup>31b</sup> the latter covering catalysts very similar to our Pd precatalyst **A4**.

When testing Pd complexes in Suzuki–Miyaura coupling catalysis, it is certainly essential to consider earlier findings of Pd nanoparticles or traces of metallic Pd in the used basic salts being able to catalyze the reaction between arylbromides and boronic acids.<sup>32</sup> In order to find optimum reaction conditions, we undertook preliminary catalytic examinations with 4-bromoacetophenone as substrate. However, yields above 99% were common in this reaction and thwarted distinction between subtle improvements in yields through variation of base or solvent. To allow for better distinction, we chose 4-chloroacetophenone as substrate to find the best reaction conditions (see Supporting Information).

With the supposedly ideal reaction conditions found, we decided to shift our focus on using the more reactive arylbromides as substrates for Suzuki–Miyaura coupling under mild conditions. Table 3 provides an overview of the tested substrates and obtained yields. 4-Bromoacetophenone gave quantitative yields under the tested conditions and allowed for a reduced reaction time of 12 h (Table 3, entry 7). However, apart from this rather reactive congener, also less reactive arylbromide substrates were tested and gave good to quantitative yields within 12 h at a reaction temperature of  $65^\circ\text{C}$ . In this comparison of substrates, lowest yields were obtained for mesityl bromide (22%) and 4-bromoanisole (67%) (Table 3, entries 3 and 4). The appearance of Pd nanoparticles was tested by poisoning experiments using mercury (entry 8).

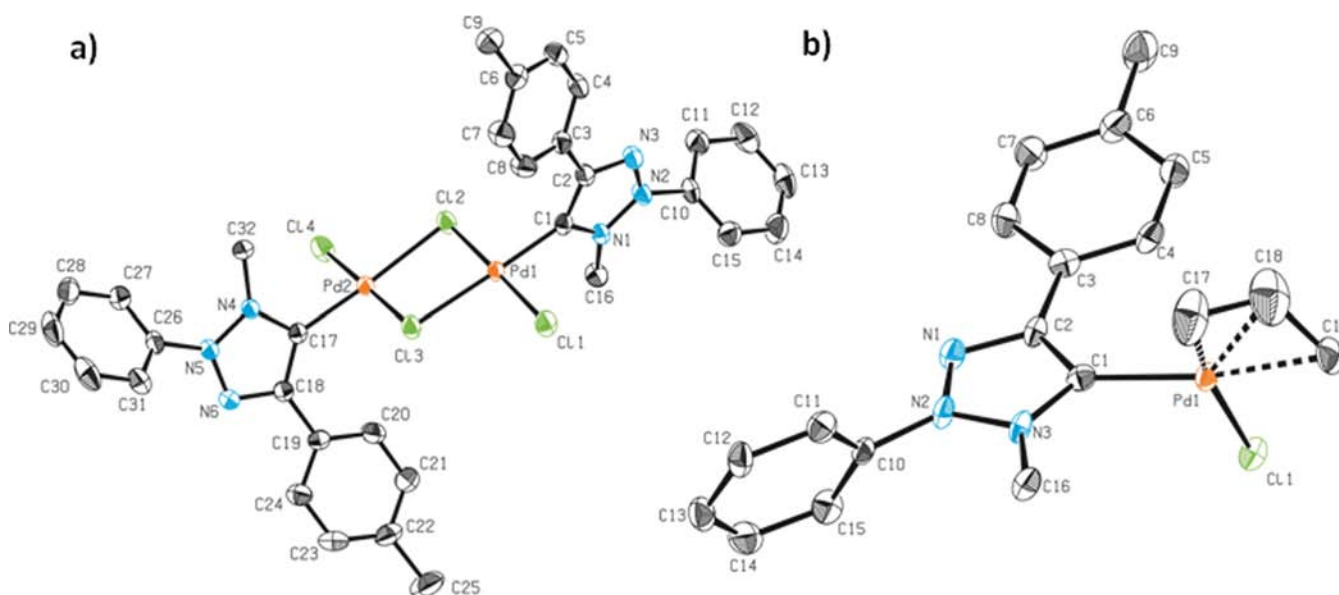


**Figure 6.** ORTEP representation (thermal ellipsoids are shown at a probability level of 50%) of the structure of (a) earlier described Cl-bridged homo-bimetallic Pd complex. Selected bond distances [Å] and angles [deg]: C1–Pd1 1.963(2), Pd1–Cl1 2.278(1), Pd1–Cl2 2.334(1), Cl1–Pd1–C1 88.15(6), Cl2–Pd1–C1 91.97(6). (b) Compound A4. Peaks of residual electron density could not be assigned adequately; therefore, no geometrical parameters are discussed.

As a result, severely reduced yields were detected, suggesting that the catalytically active species were at least in part Pd nanoparticles and **A4** exhibiting limited stability.

Reaction with chloride substrates gave a maximum of 56% yield when using the comparably more reactive 4-chloroacetophenone as substrate and using prolonged reaction times (even a long time experiment over 48 h was conducted). Furthermore,  $^1\text{H}$  NMR proved that unidentifiable side products (8%) were obtained in the reaction as well. On the basis of the observed low yields in the examinations utilizing 4-chloroacetophenone as substrate, we estimate that other, less reactive, aryl chloride substrates would give even lower yields. On that account, further examinations with these substrates were not undertaken.

The results of our initial evaluations of a Pd complex with normal 1,2,3-triazolylidene ligands in Suzuki–Miyaura coupling catalysis allow for classification of **A4** as a mediocre performing catalyst. Observed formation of Pd nanoparticles and incomplete conversion of the tested aryl chloride substrate provides evidence for a limited stability of **A4** under catalytic conditions. Therefore, results obtained are likely to reflect the observations made by Albrecht and co-workers.<sup>9j</sup> We also observed that the catalytic performance of our compound in the Suzuki–Miyaura coupling of aryl chlorides is closely related to its stability under catalytic conditions. Accordingly, alkyl substituents at the N1 position of the heterocyclic ligands are not likely to improve stability, and therefore, they should be excluded when designing new ligand generations. The report of Fukuzawa et al.<sup>31b</sup> provided evidence that a substitution pattern containing aryl substituents at positions 1 and 4 of the heterocyclic ligand drastically improves performance. This observation was generally described by Bertrand and Grubbs.<sup>10f</sup> Consequently, changing our substitution pattern to a 1,2,4-triaryl substitution in combination with replacing the Pd-bound allyl ligand to a cinnamyl ligand are both measures likely to bring great improvements in terms of stability and hence performance for prospective Pd catalysts.

## CONCLUSION

Hitherto underexplored ‘normal’ triazolylidenes are viable ligands for transition metal complexes. Synthesis of new metal compounds via the convenient silver carbene transmetalation route is possible and allows complex isolation in high yields. Applications of newly isolated triazolylidene compounds **A3** (Mo) and **A4** (Pd) in catalysis were examined, for example, epoxidation catalysis of alkenes and Suzuki–Miyaura coupling of aryl bromides and chlorides.

In the case of Pd-promoted Suzuki–Miyaura CC-coupling catalysis, stability issues prevent more successful catalytic application. Here, our examinations highlighted the drawbacks of the present N1-alkyl ligand design. It is highly likely that a triaryl substitution pattern will help to improve ligand stability of ‘normal’ 1,2,3-triazolylidenes as it was described for abnormal triazolylidenes in the literature. For this reason, current research efforts in our laboratories focus on variation of these novel ligands’ substitution pattern in order to reveal their full synthetic and catalytic potential.

## EXPERIMENTAL SECTION

**Materials.** All preparations and manipulations were performed under argon atmosphere using standard Schlenk techniques or in a glovebox. All glassware was dried in an oven at 80 °C overnight and further flame dried in vacuo before use. THF was dried over sodium/benzophenone with subsequent distillation. All other solvents were dried with a MBraun MB SPS purification system and degassed via repeated freeze–pump–thaw cycles. All commercial compounds were used without further purification. 1-Methyl-2-phenyl-4-*p*-tolyl-1,2,3-triazolium-chloride and 1-cyclohexyl-2-phenyl-4-*p*-tolyl-1,2,3-triazolium-chloride were prepared following procedures described in the literature.<sup>13</sup>

**Instruments.**  $^1\text{H}$  and  $^{13}\text{C}\{^1\text{H}\}$  NMR spectra were recorded on a 400 MHz Bruker Avance III or a 400 MHz Bruker Avance DPX spectrometer at a temperature of 298 K if not indicated otherwise. Spectra were referenced in parts per million (ppm) with an internal standard using the residual solvent shifts. Abbreviations for signal multiplicities are singlet (s), doublet (d), triplet (t), quartet (q), multiplet (m), broad (br). IR spectra were recorded on a Varian 670

**Table 3. Substrate Scope of A4 in Suzuki–Miyaura Coupling Catalysis**

Entry	Aryl halide	Product	Yield(%)
1 <sup>a</sup>			>99 <sup>b</sup>
2 <sup>a</sup>			>99 <sup>b</sup>
3 <sup>a</sup>			22 <sup>b</sup>
4 <sup>a</sup>			67 <sup>b</sup>
5 <sup>a</sup>			92 <sup>c</sup>
6 <sup>a</sup>			97 <sup>b</sup>
7 <sup>a</sup>			>99 <sup>b</sup>
8 <sup>f</sup>			8
9 <sup>d</sup>			56 <sup>b</sup>
10 <sup>e</sup>			8 <sup>b</sup>

<sup>a</sup>Reaction conditions: 1.0 mmol of aryl halide, 2.0 mmol of arylboronic acid, 2.0 mmol of Cs<sub>2</sub>CO<sub>3</sub>, 1 mol % A4, 65 °C, 12 h. <sup>b</sup>NMR yields, average of two runs. <sup>c</sup>Isolated yield. <sup>d</sup>2 mol % A4 was used, 24 h. <sup>e</sup>2.0 mmol of Cs<sub>2</sub>CO<sub>3</sub>, 1.5 mL of dioxane, 1 mol % A4, 100 °C, 24 h. <sup>f</sup>Same reaction conditions as in entry 4, except that 3 g of mercury was added after 5 min of reaction time.

FT-IR Spectrometer. ESI-HRMS analysis was performed on a Thermo Scientific LTQ Orbitrap XL by Thermo Fisher Scientific. Elemental analyses were conducted by the microanalytical laboratory of the Technical University of Munich.

**Single-Crystal X-ray Structure Determinations.** Data were collected on an X-ray single-crystal diffractometer equipped with a CCD detector (Bruker APEX II,  $\kappa$ -CCD), a fine focus sealed tube with Mo K $\alpha$  radiation ( $\lambda = 0.71073$  Å), and a graphite monochromator using the APEX 2 software package.<sup>33</sup> Measurements were performed on a single crystal coated with perfluorinated ether. The crystal was fixed on the top of a glass fiber and transferred to the diffractometer. The crystal was frozen under a stream of cold nitrogen. A matrix scan was used to determine the initial lattice parameters. Reflections were merged and corrected for Lorentz and polarization effects, scan speed, and background using SAINT.<sup>34</sup> Absorption corrections, including odd- and even-ordered spherical harmonics, were performed using SADABS.<sup>34</sup> Space group assignments were based upon systematic absences, E statistics, and successful refinement of the structures, Table 4. Structures were solved by direct methods with the aid of successive difference Fourier maps<sup>33</sup> and refined against all data using SHELXL-97<sup>35</sup> in conjunction with SHELXL.<sup>36</sup> If not mentioned otherwise, non-hydrogen atoms were refined with anisotropic displacement parameters. Hydrogen atoms were placed in ideal positions using the SHELXL riding model. Full-matrix least-squares refinements were carried out by minimizing  $\sum w(F_o^2 - F_c^2)^2$  with the SHELXL-97<sup>35</sup>

weighting scheme. Neutral atom scattering factors for all atoms and anomalous dispersion corrections for the non-hydrogen atoms were taken from the *International Tables for Crystallography*.<sup>37</sup> Images of the crystal structures were generated by PLATON.<sup>38</sup>

Crystallographic data (excluding structure factors) for the structures reported in this paper have been deposited with the Cambridge Crystallographic Data Centre as supplementary publication numbers CCDC-918410 (chloroform adduct), CCDC-918406 (A1), CCDC-918408 (B2), CCDC-918407 (A3), and CCDC-918409 (bridged Pd complex). Copies of the data can be obtained free of charge on application to the CCDC, 12 Union Road, Cambridge CB2 1EZ, U.K. (fax (+44)1223-336-033; e-mail deposit@ccdc.cam.ac.uk).

**(1-Methyl-2-phenyl-4-tolyl-1,2,3-triazol-5-ylidene)silver(I) Chloride (A1).** Under argon atmosphere, 20 mL of anhydrous dichloromethane were added to a Schlenk tube charged with 1-methyl-2-phenyl-4-*p*-tolyl-1,2,3-triazolium chloride (0.500 g, 1.75 mmol, 1.00 equiv) and silver(I) oxide (0.203 g, 0.880 mmol, 0.50 equiv). The reaction solution was stirred at room temperature under exclusion of light for 2 h. Then, the mixture was filtered through Celite to give a pale yellow solution. The solution was concentrated, and diethyl ether was added to afford a white precipitate. After filtration, a white solid (0.42 g, 63.0%) was obtained.

<sup>1</sup>H NMR (400 MHz, CDCl<sub>3</sub>)  $\delta$  (ppm): 8.04 (d, <sup>3</sup>J<sub>HH</sub> = 8.2 Hz, 2H, CH<sub>ar</sub>), 7.72–7.64 (m, 3H, CH<sub>ar</sub>), 7.59 (dd, <sup>3</sup>J<sub>HH</sub> = 7.9, 1.8 Hz, 2H, CH<sub>ar</sub>), 7.20 (d, <sup>3</sup>J<sub>HH</sub> = 8.0 Hz, 2H, CH<sub>ar</sub>), 4.29 (s, 3H, NCH<sub>3</sub>), 2.37 (s, 3H, CCH<sub>3</sub>). <sup>13</sup>C{<sup>1</sup>H} NMR (101 MHz, CDCl<sub>3</sub>)  $\delta$  (ppm): 170.6 (Ag–C<sub>trz</sub>), 157.0 (C<sub>trz</sub>), 139.6, 135.5, 132.0, 130.4, 129.7, 127.7, 126.7, 126.5 (all C<sub>ar</sub>), 42.6 (NCH<sub>3</sub>), 24.5 (CCH<sub>3</sub>). MS (FAB) *m/z* (%): 355.8 [M]<sup>+</sup>. MS (ESI) *m/z* (%): 356 [M]<sup>+</sup>, 250.2 [Trz + H]<sup>+</sup>. Anal. Calcd for C<sub>16</sub>H<sub>15</sub>AgClN<sub>3</sub> (391.00): C, 48.94; H, 3.85; N, 10.70; Cl, 9.03. Found: C, 48.99; H, 3.87; N, 10.72; Cl, 8.5.

**(1-Cyclohexyl-2-phenyl-4-tolyl-1,2,3-triazol-5-ylidene)silver(I) Chloride (B1).** Under argon atmosphere, 15 mL of a 1:1 mixture of acetonitrile and dichloromethane (anhydrous) were added to a Schlenk tube charged with 1-cyclohexyl-2-phenyl-4-*p*-tolyl-1,2,3-triazolium-chloride (0.096 g, 0.30 mmol, 1.00 equiv), silver(I) oxide (0.104 g, 0.45 mmol, 1.50 equiv), and 3 Å molecular sieves. The reaction solution was stirred at room temperature under exclusion of light for 18 h. After filtration, the brown solution was concentrated and 8 mL of diethyl ether was added to give a brown precipitate. The crude product was washed with diethyl ether twice to obtain an off-white solid (0.15 g, 25.0%).

<sup>1</sup>H NMR (400 MHz, CD<sub>2</sub>Cl<sub>2</sub>)  $\delta$  (ppm): 8.10 (d, <sup>3</sup>J<sub>HH</sub> = 8.1 Hz, 2H, CH<sub>ar</sub>), 7.82–7.63 (m, 3H, CH<sub>ar</sub>), 7.49 (d, <sup>3</sup>J<sub>HH</sub> = 7.0 Hz, 2H, CH<sub>ar</sub>), 7.31 (d, <sup>3</sup>J<sub>HH</sub> = 8.0 Hz, 2H, CH<sub>ar</sub>), 4.38 (tt, <sup>3</sup>J<sub>HH</sub> = 11.6, 3.7 Hz, 1H, NCH), 2.48 (pseudo-qd, <sup>2</sup>J<sub>HH</sub> = 13.1, <sup>3</sup>J<sub>HH</sub> = 3.7 Hz, 2H, CCH<sub>2</sub>), 2.41 (s, 3H, CCH<sub>3</sub>), 2.09 (d, <sup>3</sup>J<sub>HH</sub> = 11.3 Hz, 2H, CCH<sub>2</sub>), 1.99 (m, 2H, CCH<sub>2</sub>), 1.69 (d, <sup>3</sup>J<sub>HH</sub> = 13.0 Hz, 1H, CCH<sub>2</sub>), 1.40–1.19 (m, 3H, CCH<sub>2</sub>). <sup>13</sup>C{<sup>1</sup>H} NMR (101 MHz, CD<sub>2</sub>Cl<sub>2</sub>)  $\delta$  (ppm): 163.8 (Ag–C<sub>trz</sub>), 157.8 (C<sub>trz</sub>), 140.3, 135.4, 132.7, 131.0, 130.2, 129.0, 127.4, 127.3, (all C<sub>ar</sub>), 62.5 (NCH), 35.86 (NCH<sub>3</sub>), 26.07 (CCH<sub>2</sub>), 25.2 (CCH<sub>2</sub>), 21.6 (CCH<sub>3</sub>). MS (ESI) *m/z* (%): 742.5 [M – Cl + Trz]<sup>+</sup>, 423.8 [M – Cl]<sup>+</sup>, 318.0 [Trz + H]<sup>+</sup>.

**(1-Methyl-2-phenyl-4-tolyl-1,2,3-triazol-5-ylidene)rhodium(I) Chloride (A2).** Under argon atmosphere, 3 mL of anhydrous dichloromethane were added as solvent to a Schlenk tube charged with A1 (0.0500 g, 0.127 mmol, 2.00 equiv) and [Rh(COD)Cl]<sub>2</sub> (0.0316 g, 0.064 mmol, 1.00 equiv). The reaction solution was stirred at room temperature under exclusion of light for 2 h. Then the reaction mixture was filtered to give an orange solution. The solution was concentrated, and 5 mL of pentane was added to give a yellow precipitate. The crude product was washed twice with pentane to obtain a yellow solid (0.0586 g, 93.0%).

Obtained data are in accordance with literature values.<sup>12</sup>

**(1-Cyclohexyl-2-phenyl-4-tolyl-1,2,3-triazol-5-ylidene)rhodium(I) Chloride (B2).** Under argon atmosphere, 3 mL of anhydrous dichloromethane were added to a Schlenk tube charged with B1 (0.0500 g, 0.109 mmol, 2.00 equiv) and [Rh(COD)Cl]<sub>2</sub> (0.0268 g, 0.054 mmol, 1.00 equiv). The reaction solution was stirred at room temperature under exclusion of light for 2 h. Then the



Table 4. Crystallographic Data for Compounds: CHCl<sub>3</sub> Adduct, A1, A3, B2, and the  $\mu$ -Chloro-Bridged Pd Complex

	CHCl <sub>3</sub> adduct	A1	A3	B2	$\mu$ -Cl Pd complex
formula	C <sub>17</sub> H <sub>16</sub> Cl <sub>3</sub> N <sub>3</sub>	C <sub>16</sub> H <sub>15</sub> AgClN <sub>3</sub>	C <sub>23</sub> H <sub>20</sub> ClMoN <sub>3</sub> O <sub>2</sub>	C <sub>29</sub> H <sub>35</sub> ClN <sub>3</sub> Rh	C <sub>32</sub> H <sub>30</sub> Cl <sub>4</sub> N <sub>6</sub> Pd <sub>2</sub>
fw	368.68	392.63	501.81	563.96	853.22
color/habit	pale yellow/fragment	colorless/fragment	orange-red/fragment	red/fragment	orange/fragment
cryst dimens (mm <sup>3</sup> )	0.20 × 0.20 × 0.20	0.04 × 0.05 × 0.52	0.06 × 0.16 × 0.58	0.05 × 0.20 × 0.20	0.04 × 0.13 × 0.25
cryst syst	orthorhombic	triclinic	monoclinic	monoclinic	monoclinic
space group	<i>Pca</i> 2 <sub>1</sub> (no.29)	<i>P</i> 1 (no. 2)	<i>P</i> 2 <sub>1</sub> / <i>c</i> (no. 14)	<i>P</i> 2 <sub>1</sub> / <i>c</i> (no. 14)	<i>P</i> 2 <sub>1</sub> / <i>n</i> (no. 14)
<i>a</i> , Å	20.6804(9)	5.9205(2)	14.9104(5)	10.1793(3)	11.9638(10)
<i>b</i> , Å	8.2500(4)	12.1256(6)	11.4808(4)	19.8096(7)	11.5099(11)
<i>c</i> , Å	10.0422(4)	12.4065(6)	14.0996(5)	13.1890(5)	24.084(2)
$\alpha$ , deg	90	115.183(2)	90	90	90
$\beta$ , deg	90	101.493(2)	115.127(1)	98.846(2)	95.061(4)
$\gamma$ , deg	90	90.792(2)	90	90	90
<i>V</i> , Å <sup>3</sup>	1713.33(13)	784.95(6)	2185.21(13)	2627.90(16)	3303.5(5)
<i>Z</i>	4	2	4	4	4
<i>T</i> , K	173	123	123	173	173
<i>D</i> <sub>calcd</sub> , g cm <sup>-3</sup>	1.429	1.661	1.525	1.426	1.715
$\mu$ , mm <sup>-1</sup>	0.537	1.450	0.747	0.774	1.445
<i>F</i> (000)	760	392	1016	1168	1696
$\theta$ range, deg	1.97 – 25.32	1.86 – 25.46	1.51 – 25.38	2.02 – 26.34	1.70 – 25.35
index ranges ( <i>h</i> , <i>k</i> , <i>l</i> )	–24 – 16, $\pm$ 9, $\pm$ 12	$\pm$ 7, $\pm$ 14, $\pm$ 14	$\pm$ 17, $\pm$ 13, –13 – 16	$\pm$ 12, –24 – 22, –15 – 16	$\pm$ 14, $\pm$ 13, $\pm$ 28
no. of reflns collected	32 306	16 030	22 712	50 409	70 917
no. of indep reflns/ <i>R</i> <sub>int</sub>	3126/0.0251	2872/0.0485	3974/0.0630	5347/0.0369	6019/0.0359
no. of obsd reflns ( <i>I</i> > 2 $\sigma$ ( <i>I</i> ))	3070	2302	2845	4683	5352
no. of data/restraints/params	3126/1/272	2872/0/192	3974/0/273	5347/0/308	6019/0/401
<i>R</i> <sub>1</sub> / <i>wR</i> <sub>2</sub> ( <i>I</i> > 2 $\sigma$ ( <i>I</i> )) <sup>a</sup>	0.0180/0.0482	0.0297/0.0528	0.0356/0.0671	0.0220/0.0623	0.0194/0.0451
<i>R</i> <sub>1</sub> / <i>wR</i> <sub>2</sub> (all data) <sup>a</sup>	0.0188/0.0489	0.0494/0.0582	0.0685/0.0774	0.0288/0.0665	0.0245/0.0477
GOF (on <i>F</i> <sup>2</sup> ) <sup>a</sup>	1.084	0.976	1.021	0.989	1.050
largest diff peak and hole (e Å <sup>-3</sup> )	+0.16/–0.16	+0.43/–0.38	+0.62/–0.64	+0.40/–0.40	+0.30/–0.33

<sup>a</sup>*R*<sub>1</sub> =  $\Sigma(|F_o| - |F_c|)/\Sigma F_o$ ; *wR*<sub>2</sub> =  $\{\Sigma[w(F_o^2 - F_c^2)^2]/\Sigma[w(F_o^2)]\}^{1/2}$ ; GOF =  $\{\Sigma[w(F_o^2 - F_c^2)^2]/(n - p)\}^{1/2}$ .

reaction mixture was filtered to give an orange solution. The solution was concentrated, and pentane was added to give a red precipitate. The crude product was washed twice with pentane to obtain a dark red solid (0.0473 g, 77.0%).

<sup>1</sup>H NMR (400 MHz, CDCl<sub>3</sub>)  $\delta$  (ppm): 8.80 (d, <sup>3</sup>*J*<sub>HH</sub> = 8.1 Hz, 2H, CH<sub>ar</sub>), 7.68–7.53 (m, 3H, CH<sub>ar</sub>), 7.39 (d, <sup>3</sup>*J*<sub>HH</sub> = 7.3 Hz, 2H, CH<sub>ar</sub>), 7.32 (d, <sup>3</sup>*J*<sub>HH</sub> = 8.0 Hz, 2H, CH<sub>ar</sub>), 5.44 (tt, <sup>3</sup>*J*<sub>HH</sub> = 12.1, 3.2 Hz, 1H, CCH), 5.24–4.98 (m, 2H, COD), 3.20–3.10 (m, 1H, COD), 3.07–3.00 (m, 1H, COD), 2.70 (pseudo-qd, <sup>2</sup>*J*<sub>HH</sub> = 12.3, <sup>3</sup>*J*<sub>HH</sub> = 3.5 Hz, 1H, CCH<sub>2</sub>), 2.54 (pseudo-qd, <sup>2</sup>*J*<sub>HH</sub> = 12.5, <sup>3</sup>*J*<sub>HH</sub> = 3.6 Hz, 1H, CCH<sub>2</sub>), 2.43 (s, 3H, CCH<sub>3</sub>), 2.42–2.22 (m, 4H, COD), 2.13 (tdd, <sup>2</sup>*J*<sub>HH</sub> = 15.8, <sup>3</sup>*J*<sub>HH</sub> = 11.0, 8.1 Hz, 2H, COD), 2.04–1.81 (m, 5H, COD and CCH<sub>2</sub>), 1.70 (t, <sup>3</sup>*J*<sub>HH</sub> = 13.0 Hz, 2H, COD), 1.52–1.09 (m, 4H, CCH<sub>2</sub>). <sup>13</sup>C{<sup>1</sup>H} NMR (101 MHz, CDCl<sub>3</sub>)  $\delta$  (ppm): 181.1 (Rh–C<sub>tr</sub>), 155.7 (C<sub>tr</sub>), 138.8 (C<sub>tr</sub>), 137.4, 131.7, 129.9, 129.0, 128.9, 128.8, 127.8 (all C<sub>ar</sub>), 96.7, 96.6, 96.5, 96.4 (all C<sub>OD</sub>), 71.5, 71.3, 67.9, 67.8, 66.2, 66.0, 34.2, 33.3, 32.7, 32.6, 29.8, 28.7, 26.4, 26.3, 25.2, 21.6, 15.4. MS (FAB) *m/z* (%): 562.4 [M]<sup>+</sup>, 527.5 [M – Cl]<sup>+</sup>, 418.5 [M – COD – Cl]<sup>+</sup>, 317.8 [Trz + H]<sup>+</sup>. MS (ESI) *m/z* (%): 528.0 [M – Cl]<sup>+</sup>, 419.2 [M – Cl – COD]<sup>+</sup>. Anal. Calcd for C<sub>29</sub>H<sub>35</sub>RhClN<sub>3</sub> (563.16): C, 61.76; H, 6.26; N, 7.45. Found: C, 61.89; H, 6.27; N, 7.33.

**(1-Methyl-2-phenyl-4-tolyl-1,2,3-triazol-5-ylidene) molybdenum Dicarboxylate (A3).** Under argon atmosphere, 20 mL of anhydrous dichloromethane were added to a mixture of A1 (0.300 g, 0.764 mmol, 1.00 equiv) and [Mo(CO)<sub>3</sub>CpCl] (0.215 g, 0.764 mmol, 1.00 equiv) inside a Schlenk flask. The reaction was heated to reflux for 16 h under exclusion of light. Then the reaction mixture was passed through Celite to give a dark red solution. After concentrating the solution, hexane was added to precipitate the crude product. A red solid (0.254 g, 63.9%) was obtained by recrystallization from dichloromethane and hexane.

<sup>1</sup>H NMR (400 MHz, CD<sub>2</sub>Cl<sub>2</sub>)  $\delta$  (ppm): 7.67–7.59 (m, 3H, CH<sub>ar</sub>), 7.51 (dd, <sup>3</sup>*J*<sub>HH</sub> = 6.8, 2.9 Hz, 2H, CH<sub>ar</sub>), 7.43 (d, <sup>3</sup>*J*<sub>HH</sub> = 8.0 Hz, 2H, CH<sub>ar</sub>), 7.35 (d, <sup>3</sup>*J*<sub>HH</sub> = 7.9 Hz, 2H, CH<sub>ar</sub>), 5.13 (s, 5H, H<sub>CP</sub>), 4.03 (s,

3H, NCH<sub>3</sub>), 2.46 (s, 3H, CCH<sub>3</sub>). <sup>13</sup>C{<sup>1</sup>H} NMR (101 MHz, CD<sub>2</sub>Cl<sub>2</sub>)  $\delta$  (ppm): 258.8 (CO), 253.2 (CO), 185.8 (Mo–C<sub>tr</sub>), 159.4 (C<sub>tr</sub>), 140.1, 136.4, 131.9, 131.4, 130.6, 130.5, 129.6, 126.5 (all C<sub>ar</sub>), 96.48 (C<sub>CP</sub>), 41.6 (NCH<sub>3</sub>), 21.72 (CCH<sub>3</sub>). IR (solid):  $\nu$  = 1943, 1848 ( $\nu$ (CO)) cm<sup>-1</sup>. MS (ESI) *m/z* (%): 468.0 [M – Cl]<sup>+</sup>. Anal. Calcd for C<sub>23</sub>H<sub>20</sub>ClMoN<sub>3</sub>O<sub>2</sub> (503.0): C, 55.05; H, 4.02; N, 8.37. Found: C, 55.03; H, 4.27; N, 8.30.

**(1-Methyl-2-phenyl-4-tolyl-1,2,3-triazolylidene) allylpalladium(II) Chloride (A4).** Under argon atmosphere, 5 mL of anhydrous dichloromethane were added as solvent to allylpalladium(II) chloride (0.070 g, 0.191 mmol, 1.00 equiv) and A1 (0.150 g, 0.383 mmol, 2.00 equiv) in a Schlenk tube. The reaction was stirred at room temperature under exclusion of light for 16 h. The reaction mixture was filter through cannula with the Schlenk technique. All volatiles were evaporated, and the residue was washed with hexane. An off-white solid (0.060 g, 67.9%) was obtained after removal of hexane.

<sup>1</sup>H NMR (400 MHz, CDCl<sub>3</sub>)  $\delta$  (ppm): 8.18 (d, <sup>3</sup>*J*<sub>HH</sub> = 8.1 Hz, 2H, CH<sub>ar</sub>), 7.78–7.60 (m, 3H, CH<sub>ar</sub>), 7.53 (dd, <sup>3</sup>*J*<sub>HH</sub> = 6.4, 3.0 Hz, 2H, CH<sub>ar</sub>), 7.23 (d, <sup>3</sup>*J*<sub>HH</sub> = 8.0 Hz, 2H, CH<sub>ar</sub>), 5.35 (m, 1H, allyl), 4.39 (s, 3H, NCH<sub>3</sub>), 4.36 (d, <sup>3</sup>*J*<sub>HH</sub> = 7.5 Hz, 1H, allyl), 3.38 (d, <sup>3</sup>*J*<sub>HH</sub> = 13.6 Hz, 1H, allyl), 3.16 (d, <sup>3</sup>*J*<sub>HH</sub> = 6.4 Hz, 1H, allyl), 2.39 (s, 3H, CCH<sub>3</sub>), 2.36 (d, <sup>3</sup>*J*<sub>HH</sub> = 12.0 Hz, 1H, allyl). <sup>13</sup>C{<sup>1</sup>H} NMR (101 MHz, CDCl<sub>3</sub>)  $\delta$  (ppm): 174.8 (Pd–C<sub>tr</sub>), 156.9 (C<sub>tr</sub>), 139.1, 135.8, 131.5, 130.3, 129.2, 128.7, 127.9, 126.4 (all C<sub>ar</sub>), 115.1 (CCH<sub>2</sub>), 72.8 (CCH), 50.3 (CCH<sub>2</sub>), 41.0 (NCH<sub>3</sub>), 21.5 (CCH<sub>3</sub>). MS (FAB) *m/z* (%): 645.1 [M – Cl + Trz]<sup>+</sup>, 436.8 [M – Pd + 2allyl]<sup>+</sup>, 395.0 [M – Cl]<sup>+</sup>, 250.3 [Trz]<sup>+</sup>. MS (ESI) *m/z* (%): 644.2 [M – Cl + Trz]<sup>+</sup>, 395.5 [M – Cl]<sup>+</sup>, 249.9 [Trz + H]<sup>+</sup>. Anal. Calcd for C<sub>19</sub>H<sub>20</sub>ClN<sub>3</sub>Pd: C, 52.79; H, 4.66; N, 9.72; Cl, 8.20. Found: C, 52.39; H, 4.74; N, 9.63; Cl, 8.7.

***p*-Cymene-(1-methyl-2-phenyl-4-tolyl-1,2,3-triazolylidene) ruthenium(II) Dichloride (A5).** Under argon atmosphere, 5 mL of anhydrous dichloromethane were added to a mixture of [RuCl<sub>2</sub>(*p*-cymene)]<sub>2</sub> (0.078 g, 0.127 mmol, 1.00 equiv) and A1 (0.100 g, 0.255 mmol, 2.00 equiv) in a Schlenk tube. The reaction was stirred at room

temperature under exclusion of light for 2 h. The reaction mixture was filtered through silica gel, and the complex was washed down with acetone. Removal of acetone afforded the crude product. Then, acetone was used for recrystallization to obtain a dark red solid (0.097 g, 68.7%).

$^1\text{H}$  NMR (400 MHz,  $\text{CDCl}_3$ )  $\delta$  (ppm): 7.98 (d,  $^3J_{\text{HH}} = 8.0$  Hz, 2H,  $\text{CH}_{\text{ar}}$ ), 7.69–7.58 (m, 3H,  $\text{CH}_{\text{ar}}$ ), 7.52 (d,  $^3J_{\text{HH}} = 5.2$  Hz, 2H,  $\text{CH}_{\text{ar}}$ ), 7.25 (d, 2H,  $\text{CH}_{\text{ar}}$ ), 5.20 (d,  $^3J_{\text{HH}} = 5.8$  Hz, 2H, cymene-CH), 4.93 (d,  $^3J_{\text{HH}} = 5.7$  Hz, 2H, cymene-CH), 4.41 (s, 3H,  $\text{NCH}_3$ ), 2.75 [dt,  $^3J_{\text{HH}} = 14.2$ , 7.2 Hz, 1H, cymene- $\text{C}(\text{CH}_3)_2$ ], 2.42 (s, 3H,  $\text{CCH}_3$ ), 2.01 (s, 3H,  $\text{CCH}_3$ ), 1.18 [d,  $^3J_{\text{HH}} = 6.9$  Hz, 6H, cymene- $\text{C}(\text{CH}_3)_2$ ].  $^{13}\text{C}\{^1\text{H}\}$  NMR (101 MHz,  $\text{CDCl}_3$ )  $\delta$  (ppm): 173.4 (Ru- $\text{C}_{\text{trz}}$ ), 160.75 ( $\text{C}_{\text{trz}}$ ), 138.9, 135.8, 131.5, 130.8, 130.2, 130.1, 128.6, 126.6 (all  $\text{C}_{\text{ar}}$ ), 106.6, 100.3, 86.1, 84.3 (all  $\text{C}_{\text{cym}}$ ), 42.2 ( $\text{NCH}_3$ ), 31.0 [ $\text{C}(\text{CH}_3)_2$ ], 22.7 [2C,  $\text{C}(\text{CH}_3)_2$ ], 21.5 (tolyl- $\text{CH}_3$ ), 18.8 (cymene- $\text{CH}_3$ ). MS (FAB)  $m/z$  (%): 655.4 [ $\text{M} + \text{Ru}$ ] $^+$ , 521.4 [ $\text{M} - \text{Cl}$ ] $^+$ , 483.5 [ $\text{M} - 2\text{Cl}$ ] $^+$ , 249.9 [ $\text{Trz} + \text{H}$ ] $^+$ . MS (ESI)  $m/z$  (%): 520.0 [ $\text{M} - \text{HCl}$ ] $^+$ , 484.1 [ $\text{M} - 2\text{HCl}$ ] $^+$ . Anal. Calcd for  $\text{C}_{26}\text{H}_{29}\text{Cl}_2\text{N}_3\text{Ru}$ : C, 56.22; H, 5.26; N, 7.56; Cl, 12.76; Ru, 18.19. Found: C, 56.50; H, 5.24; N, 7.81; Cl, 12.33.

#### Procedures for Oxidation in Epoxidation Catalysis.

All catalytic reactions were performed under laboratory atmosphere (under air at RT) in a reaction vessel equipped with a magnetic stirrer.

**cis-Cyclooctene.** Olefin (800 mg, 7.3 mmol) and catalyst (1 mol %, 73  $\mu\text{mol}$ ) dissolved in RTIL (0.5 mL) were added to the reaction vessel. Afterwards, the reaction was initiated by adding TBHP (2.65 mL, 5.5  $m$  in *n*-decane). Analysis: The course of the reaction was monitored by quantitative GC analysis. Samples taken were treated with  $\text{MgSO}_4$  and  $\text{MnO}_2$  to remove water and destroy excess peroxide. Afterward, the sample was diluted with  $\text{CH}_2\text{Cl}_2$  and the resulting slurry was filtered. A mixture of 4 mg/mL indane and *p*-xylol in isopropanol (used as external standard) and the filtrate was injected into a GC column. Conversion of *cis*-cyclooctene and formation of the respective oxides were calculated from calibration curves ( $r^2 > 0.999$ ) recorded prior to the start of the reaction.

**1-Octene.** Olefin (800 mg, 7.3 mmol), dichloroethane (7.3 mmol, internal standard), and the catalyst (1 mol %, 73  $\mu\text{mol}$ ) were added to the reaction vessel and diluted in RTIL (0.5 mL). Afterward, the reaction was initiated by adding TBHP (2.65 mL, 5.5  $m$  in *n*-decane).

**cis-Stilbene.** Olefin (0.291 g, 1.6 mmol), dichloroethane (1.6 mmol, internal standard), and catalyst (1 mol %, 16  $\mu\text{mol}$ ) were added to the reaction vessel and diluted in RTIL (0.5 mL). The reaction was initiated with addition of TBHP (0.6 mL, 5.5  $m$  in *n*-decane).

**trans- $\beta$ -Methylstyrene.** Olefin (0.118 g, 1.0 mmol), dichloroethane (1.0 mmol, internal standard), and catalyst (1 mol %, 0.01 mmol) were added to the reaction vessel and diluted in RTIL (0.5 mL). The reaction was initiated by adding TBHP (3.6 mL, 5.5  $m$  in *n*-decane).

**Analysis.** In the case of 1-octene, *trans*- $\beta$ -methylstyrene, and *cis*-stilbene the course of the reaction was monitored by NMR analysis. Samples taken were treated with  $\text{MgSO}_4$  and  $\text{MnO}_2$  to remove water and destroy excess peroxide. Afterward, the sample was diluted with  $\text{CDCl}_3$ , the resulting slurry was filtered, and the filtrate was measured.

**Recycling Experiments.** For the ongoing catalysis runs, the upper phase was removed from the reaction vessel by addition of 5 mL of *n*-hexane after cooling down to room temperature. The upper phase was removed by means of cannulation. Samples were treated with  $\text{MgSO}_4$  and  $\text{MnO}_2$  to remove water and destroy excess peroxide. Afterward, the sample was diluted with  $\text{CH}_2\text{Cl}_2$  and the resulting slurry was filtered. A mixture of 4 mg/mL indane and *p*-xylol in isopropanol (used as external standard) and the filtrate was injected into a GC column. Additionally, oil pump vacuum for 2.5 h at 55 °C allowed removal of *t*-BuOH from the remaining RTIL phase before further cyclooctene (0.800 g, 7.3 mmol) and TBHP (2.65 mL, 5.5  $m$  in *n*-decane) were added.

**General Suzuki–Miyaura Cross-Coupling Procedure.** The Pd precatalyst (0.01 or 0.02 mmol), phenylboronic acid (2.00 mmol), base (2.00 mmol), and aryl halide (1.00 mmol) were added to a Schlenk flask containing a magnetic stir bar. The vial was then purged twice with argon, and solvent (1.5 mL) was added. The reaction was stirred at the destined temperature for the desired period (see Table S2, Supporting Information, and Table 3). After reaction, the mixture

was extracted by DCM ( $2 \times 5$  mL) and filtered. The solvent of filtrate was removed in a rotary evaporator (40 °C, 100 mbar), and the crude product was directly used for chromatographic separation or dissolved by  $\text{CDCl}_3$  for  $^1\text{H}$  NMR analysis.

## ■ ASSOCIATED CONTENT

### Supporting Information

Tables of crystal parameters, atomic coordinates, bond lengths, bond angles, and thermal displacement parameters for **A1**, **A3**, **B2**,  $\text{CHCl}_3$  adduct, and the bridged Pd complex in .cif format as well as data for **A4**, for which the residual electron density is too high for further analysis; additional synthetic and catalytic experimental details, NMR spectra, as well as detailed crystallographic information. This material is available free of charge via the Internet at <http://pubs.acs.org>.

## ■ AUTHOR INFORMATION

### Corresponding Author

\*E-mail: wolfgangherrmann@ch.tum.de (W.A.H.); fritz.kuehn@ch.tum.de (F.E.K.).

### Author Contributions

$^\dagger$ Equally contributing coauthors.

### Notes

The authors declare no competing financial interest.

## ■ ACKNOWLEDGMENTS

The authors thank the Bavarian Network of Excellence: NANOCAT and the TUM Graduate School for generous financial support.

## ■ REFERENCES

- (1) (a) Öfele, K.; Herrmann, W. A.; Mihalios, D.; Elison, M.; Herdtweck, E.; Scherer, W.; Mink, J. *J. Organomet. Chem.* **1993**, 459, 177. (b) Herrmann, W. A.; Elison, M.; Fischer, J.; Köcher, C.; Öfele, K. U.S. Patent 5, 1998. (c) Crabtree, R. H. *J. Organomet. Chem.* **2005**, 690, 5451.
- (2) (a) Öfele, K. *J. Organomet. Chem.* **1968**, 12, P42. (b) Wanzlick, H. W.; Schönherr, H. *J. Angew. Chem., Int. Ed.* **1968**, 7, 141. (c) Arduengo III, A. J. U.S. Patent 5077414, 1991. (d) Herrmann, W. A. *Angew. Chem., Int. Ed.* **2002**, 41, 1290. (e) Schuster, O.; Yang, L.; Raubenheimer, H. G.; Albrecht, M. *Chem. Rev.* **2009**, 109, 3445. (f) Lin, J. C. Y.; Huang, R. T. W.; Lee, C. S.; Bhattacharyya, A.; Hwang, W. S.; Lin, I. J. B. *Chem. Rev.* **2009**, 109, 3561. (g) Arnold, P. L.; Casely, I. J. *Chem. Rev.* **2009**, 109, 3599. (h) Díez-González, S.; Marion, N.; Nolan, S. P. *Chem. Rev.* **2009**, 109, 3612. (i) Samojłowicz, C.; Bieniek, M.; Grela, K. *Chem. Rev.* **2009**, 109, 3708. (j) Burtcher, D.; Grela, K. *Angew. Chem., Int. Ed.* **2009**, 48, 442. (k) Hindi, K. M.; Panzner, M. J.; Tessier, C. A.; Cannon, C. L.; Youngs, W. J. *Chem. Rev.* **2009**, 109, 3859. (l) Schaper, L.-A.; Hock, S. J.; Herrmann, W. A.; Kühn, F. E. *Angew. Chem., Int. Ed.* **2013**, 52, 270.
- (3) Herrmann, W. A.; Elison, M.; Fischer, J.; Köcher, C.; Artus, G. R. *J. Angew. Chem., Int. Ed.* **1995**, 34, 2371.
- (4) Herrmann, W. A.; Schütz, J.; Frey, G. D.; Herdtweck, E. *Organometallics* **2006**, 25, 2437.
- (5) (a) Chianese, A. R.; Kovacevic, A.; Zeglis, B. M.; Faller, J. W.; Crabtree, R. H. *Organometallics* **2004**, 23, 2461. (b) Lavallo, V.; Canac, Y.; Präsang, C.; Donnadiu, B.; Bertrand, G. *Angew. Chem., Int. Ed.* **2005**, 44, 5705. (c) Lavallo, V.; Dyker, C. A.; Donnadiu, B.; Bertrand, G. *Angew. Chem., Int. Ed.* **2008**, 47, 5411. (d) Melaimi, M.; Parneswaran, P.; Donnadiu, B.; Frenking, G.; Bertrand, G. *Angew. Chem., Int. Ed.* **2009**, 48, 4792.
- (6) (a) Gründemann, S.; Kovacevic, A.; Albrecht, M.; Faller, R. B.; Crabtree, R. H. *Chem. Commun.* **2001**, 2274. (b) Gründemann, S.; Kovacevic, A.; Albrecht, M.; Faller, J. W.; Crabtree, R. H. *J. Am. Chem. Soc.* **2002**, 124, 10473. (c) Albrecht, M. *Chem. Commun.* **2008**, 3601.
- (7) Albrecht, M. *Chimia* **2009**, 63, 105.

- (8) (a) Mathew, P.; Neels, A.; Albrecht, M. *J. Am. Chem. Soc.* **2008**, *130*, 13534. (b) Guisado-Barrios, G.; Bouffard, J.; Donnadiou, B.; Bertrand, G. *Angew. Chem., Int. Ed.* **2010**, *49*, 4759. (c) Melaimi, M.; Soleilhavoup, M.; Bertrand, G. *Angew. Chem., Int. Ed.* **2010**, *49*, 8810. (d) Martin, D.; Melaimi, M.; Soleilhavoup, M.; Bertrand, G. *Organometallics* **2011**, *30*, 5304.
- (9) (a) Donnelly, K. F.; Petronilho, A.; Albrecht, M. *Chem. Commun.* **2013**, 1145. (b) Schuster, E. M.; Botoshansky, M.; Gandelman, M. *Dalton Trans.* **2011**, 40, 8764. (c) Poulain, A. L.; Canseco-Gonzalez, D.; Hynes-Roche, R.; Müller-Bunz, H.; Schuster, O.; Stoeckli-Evans, H.; Neels, A.; Albrecht, M. *Organometallics* **2011**, *30*, 1021. (d) Keske, E. C.; Zenkina, O. V.; Wang, R.; Crudden, C. M. *Organometallics* **2011**, *31*, 456. (e) Guisado-Barrios, G.; Bouffard, J.; Donnadiou, B.; Bertrand, G. *Organometallics* **2011**, *30*, 6017. (f) Cai, J.; Yang, X.; Arumugam, K.; Bielawski, C. W.; Sessler, J. L. *Organometallics* **2011**, *30*, 5033. (g) Kilpin, K. J.; Gavey, E. L.; McAdam, C. J.; Anderson, C. B.; Lind, S. J.; Keep, C. C.; Gordon, K. C.; Crowley, J. D. *Inorg. Chem.* **2011**, *50*, 6334. (h) Crowley, J. D.; Lee, A.-L.; Kilpin, K. J. *Aust. J. Chem.* **2011**, *64*, 1118. (i) Clough, M. C.; Zeits, P. D.; Bhuvanesh, N.; Gladysz, J. A. *Organometallics* **2012**, *31*, 5231. (j) Canseco-Gonzalez, D.; Gniewek, A.; Szulmanowicz, M.; Müller-Bunz, H.; Trzeciak, A. M.; Albrecht, M. *Chem.—Eur. J.* **2012**, *18*, 6055.
- (10) (a) Lalrempuia, R.; McDaniel, N. D.; Müller-Bunz, H.; Bernhard, S.; Albrecht, M. *Angew. Chem., Int. Ed.* **2010**, *49*, 9765. (b) Kilpin, K. J.; Paul, U. S. D.; Lee, A.-L.; Crowley, J. D. *Chem. Commun.* **2011**, 47, 328. (c) Zanardi, A.; Mata, J. A.; Peris, E. *Organometallics* **2009**, *28*, 4335. (d) Saravanakumar, R.; Ramkumar, V.; Sankararaman, S. *Organometallics* **2011**, *30*, 1689. (e) Prades, A.; Peris, E.; Albrecht, M. *Organometallics* **2011**, *30*, 1162. (f) Bouffard, J.; Keitz, B. K.; Tonner, R.; Guisado-Barrios, G.; Frenking, G.; Grubbs, R. H.; Bertrand, G. *Organometallics* **2011**, *30*, 2617.
- (11) (a) Keitz, B. K.; Bouffard, J.; Bertrand, G.; Grubbs, R. H. *J. Am. Chem. Soc.* **2011**, *133*, 8498. (b) Yan, X.; Bouffard, J.; Guisado-Barrios, G.; Donnadiou, B.; Bertrand, G. *Chem.—Eur. J.* **2012**, *18*, 14627.
- (12) Schaper, L.-A.; Öfele, K.; Kadyrov, R.; Bechlars, B.; Drees, M.; Cokoja, M.; Herrmann, W. A.; Kühn, F. E. *Chem. Commun.* **2012**, *48*, 3857.
- (13) (a) Moderhack, D.; Lorke, M. *Heterocycles* **1987**, *26*, 1751. (b) Moderhack, D.; Daoud, A. *J. Heterocycl. Chem.* **2003**, *40*, 625.
- (14) (a) Hegarty, A. F.; Kearney, J. A.; Scott, F. L. *J. Chem. Soc., Perkin Trans. 2* **1973**, 1422. (b) Rector, D. L.; Folz, S. D.; Conklin, R. D.; Nowakowski, L. H.; Kaugars, G. *J. Med. Chem.* **1981**, *24*, 532.
- (15) Schuster, R. E.; Scott, J. E.; Casanova, J. *Org. Syn.* **1966**, *46*, 75.
- (16) Ugi, I.; Meyr, R.; Lipinski, M.; Bodesheim, F.; Rosendahl, F. *Org. Syn.* **1961**, *41*, 13.
- (17) Wang, H. M. J.; Lin, I. J. B. *Organometallics* **1998**, *17*, 972.
- (18) Hintermair, U.; Englert, U.; Leitner, W. *Organometallics* **2011**, *30*, 3726.
- (19) (a) Arduengo, A. J., III; Calabrese, J. C.; Davidson, F.; Rasika Dias, H. V.; Goerlich, J. R.; Krafczyk, R.; Marshall, W. J.; Tamm, M.; Schmutzler, R. *Helv. Chim. Acta* **1999**, *82*, 2348. (b) Trnka, T. M.; Morgan, J. P.; Sanford, M. S.; Wilhelm, T. E.; Scholl, M.; Choi, T.-L.; Ding, S.; Day, M. W.; Grubbs, R. H. *J. Am. Chem. Soc.* **2003**, *125*, 2546. (c) Nyce, G. W.; Csihony, S.; Waymouth, R. M.; Hedrick, J. L. *Chem.—Eur. J.* **2004**, *10*, 4073.
- (20) Collin, R. L.; Lipscomb, W. N. *Acta Crystallogr.* **1951**, *4*, 10.
- (21) Lee, K. M.; Wang, H. M. J.; Lin, I. J. B. *J. Chem. Soc., Dalton Trans.: Inorg. Chem.* **2002**, 2852.
- (22) Bondi, A. *J. Phys. Chem.* **1964**, *68*, 441.
- (23) de Frémont, P.; Scott, N. M.; Stevens, E. D.; Ramnial, T.; Lightbody, O. C.; Macdonald, C. L. B.; Clyburne, J. A. C.; Abernethy, C. D.; Nolan, S. P. *Organometallics* **2005**, *24*, 6301.
- (24) Li, S.; Kee, C. W.; Huang, K.-W.; Hor, T. S. A.; Zhao, J. *Organometallics* **2010**, *29*, 1924.
- (25) Filippou, A. C.; Winter, J. G.; Kociok-Köhn, G.; Hinz, I. *J. Organomet. Chem.* **1997**, *542*, 35.
- (26) (a) Abrantes, M.; Santos, A. M.; Mink, J.; Kühn, F. E.; Romão, C. C. *Organometallics* **2003**, *22*, 2112. (b) Kühn, F. E.; Santos, A. M.; Abrantes, M. *Chem. Rev.* **2006**, *106*, 2455. (c) Grover, N.; Kühn, F. E. *Curr. Org. Chem.* **2012**, *16*, 16.
- (27) (a) Valente, A.; Seixas, J.; Gonçalves, I.; Abrantes, M.; Pillinger, M.; Romão, C. *Catal. Lett.* **2005**, *101*, 127. (b) Freund, C.; Abrantes, M.; Kühn, F. E. *J. Organomet. Chem.* **2006**, *691*, 3718. (c) Hauser, S. A.; Cokoja, M.; Drees, M.; Kühn, F. E. *J. Mol. Catal. A: Chem.* **2012**, *363–364*, 237. (d) Betz, D.; Raith, A.; Cokoja, M.; Kühn, F. E. *ChemSusChem* **2010**, *3*, 559. (e) Capapé, A.; Raith, A.; Herdtweck, E.; Cokoja, M.; Kühn, F. E. *Adv. Synth. Catal.* **2010**, *352*, 547. (f) Al-Ajlouni, A. M.; Veljanovski, D.; Capapé, A.; Zhao, J.; Herdtweck, E.; Calhorda, M. J.; Kühn, F. E. *Organometallics* **2008**, *28*, 639.
- (28) Abrantes, M.; Paz, F. A. A.; Valente, A. A.; Pereira, C. C. L.; Gago, S.; Rodrigues, A. E.; Klinowski, J.; Pillinger, M.; Gonçalves, I. S. *J. Organomet. Chem.* **2009**, *694*, 1826.
- (29) Kandepi, V. V. K. M.; da Costa, A. P.; Peris, E.; Royo, B. *Organometallics* **2009**, *28*, 4544.
- (30) Fu, C.-F.; Lee, C.-C.; Liu, Y.-H.; Peng, S.-M.; Warsink, S.; Elsevier, C. J.; Chen, J.-T.; Liu, S.-T. *Inorg. Chem.* **2010**, *49*, 3011.
- (31) (a) Karthikeyan, T.; Sankararaman, S. *Tetrahedron Lett.* **2009**, *50*, 5834. (b) Terashima, T.; Inomata, S.; Ogata, K.; Fukuzawa, S.-i. *Eur. J. Inorg. Chem.* **2012**, *2012*, 1387.
- (32) (a) Leadbeater, N. E.; Marco, M. *Org. Lett.* **2002**, *4*, 2973. (b) Leadbeater, N. E.; Marco, M. *J. Org. Chem.* **2003**, *68*, 5660. (c) Arvela, R. K.; Leadbeater, N. E.; Sangi, M. S.; Williams, V. A.; Granados, P.; Singer, R. D. *J. Org. Chem.* **2005**, *70*, 161.
- (33) APEX suite of crystallographic software. APEX 2, Version 2008.4; Bruker AXS Inc.: Madison, WI, 2008.
- (34) SAINT, Version 7.56a and SADABS Version 2008/1; Bruker AXS Inc.: Madison, WI, 2008.
- (35) Sheldrick, G. M. *SHELXL-97*; University of Göttingen: Göttingen, Germany, 1998.
- (36) Hübschle, C. B.; Sheldrick, G. M.; Dittrich, B. *J. Appl. Crystallogr.* **2011**, *44*, 1281.
- (37) In *International Tables for Crystallography*; Wilson, A. J. C., Ed.; Kluwer Academic Publishers: Dordrecht, The Netherlands, 1992; Vol. C, Tables 6.1.1.4, 4.2.6.8, and 4.2.4.2, , pp 500–502, 219–222, and 193–199.
- (38) Spek, A. L. *PLATON, A Multipurpose Crystallographic Tool*; Utrecht University: Utrecht, The Netherlands, 2010.